# Thermally Robust Metal Coordination Polymers: The Cobalt, Nickel, and Zinc Pyrimidin-2-olate Derivatives

**Norberto Masciocchi,*[a,b] G. Attilio Ardizzoia,*[b,c] Girolamo LaMonica,[b,c] Angelo Maspero,[b,c] and Angelo Sironi[a]**

**Keywords:** X-ray powder diffraction / Coordination chemistry / Nitrogen heterocycles / Polymers

A number of coordination polymers of the pymo ligand (Hpymo = 2-hydroxypyrimidine) have been prepared and fully characterized by chemical, spectroscopic, and thermal analyses. Their complete crystal structures have been solved ab initio from laboratory X-ray powder diffraction data and ultimately refined by the Rietveld method. The $M(pymo)_2$ species (M = Co, Ni, Zn) consist of structurally related three-dimensional frameworks of very high thermal stability (decomposing under $N_2$ only at $T > 550$ °C), with the metal atoms, linked by $\mu_2$-$\eta^1$-$\eta^1$ (*N*;*N*′) (Co, Zn) or $\mu_2$-$\eta^2$-$\eta^1$ (*N*,*O*;*N*′) bridges, about 5.4–5.7 Å apart. The hydrated species $Ni(pymo)_2(H_2O)_{2.5}$ is based on a two-dimensional array of $Ni(pymo)_2$ stoichiometry, containing both coordinated and clathrated water molecules, and can be selectively transformed into $Ni(pymo)_2$ by thermal treatment, through an amorphous intermediate, recrystallizing at $T > 315$ °C. In contrast, one dimensional chains are found in the three hydrazine adducts, $M(pymo)_2(N_2H_4)_2$, which show unique bis($\mu_2$-hydrazine) bridges (M···M ca. 4.0 Å) and terminally *O*-bonded pymo ligands.

## Introduction

Coordination polymers containing metal ions in their backbones have been widely investigated, and found to possess a variety of interesting electrical, electrochemical and optical properties.[1] In particular, metal polymers containing azoles and azolates have very recently shown remarkable magnetic,[2] anticorrosion,[3] and even antimicrobial[4] activity. In order to design stable, coordinatively saturated systems, a number of metal ions have been therefore treated with polydentate ligands, either neutral (such as 4,4′-bipyridine or longer spacers[5]) or negatively charged. In the latter group, pyrazolates[6,7] and imidazolates[8] have been found to afford binary species which could be structurally characterized only by X-ray powder diffraction (XRPD) methods.

Recently, we have shifted our interests to the less known pyrimidin-2-olate (pymo) ligand (Scheme 1), which afforded, with silver(I) ions, one-dimensional (hydrated) polymeric species[9] and cyclic hexamers,[10] and, with copper(I) ions, a surprising crystal phase containing, simultaneously, hexamers and infinite helical polymers.[11] In our search for polymers of higher dimensionality and higher thermal stability, we focused on cobalt(II), nickel(II), and zinc(II) ions, i.e. on metals with different electronic requirements, larger coordination numbers and lower redox propensities than copper and silver.

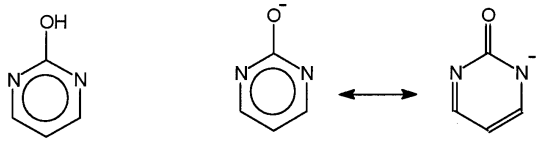

Hpymo pymo

Scheme 1

Therefore, in this paper we report on the syntheses, thermal, and spectroscopic characterization of a number of polymeric species of the M/pymo type (outlined below), which have been structurally characterized by the newly emerging ab initio XRPD technique,[12] pioneered by us in the field of coordination chemistry, from conventional laboratory equipment.[13] The following numbering scheme has been used throughout the paper: **1a** = $Co(pymo)_2$; **1b** = $Ni(pymo)_2$; **1c** = $Zn(pymo)_2$; **2b** = $Ni(pymo)_2(H_2O)_{2.5}$; **3a** = $Co(pymo)_2(N_2H_4)_2$; **3b** = $Ni(pymo)_2(N_2H_4)_2$; **3c** = $Zn(pymo)_2(N_2H_4)_2$.

## Results

### Syntheses

The reaction of 2-hydroxy-pyrimidine with cobalt, nickel, and zinc dichlorides in water, in the presence of a base such as $NH_3$, affords, in high yield, the corresponding metal pyrimidinolate derivatives $Co(pymo)_2$, **1a**, $Ni(pymo)_2(H_2O)_{2.5}$,

[a] Dipartimento di Chimica Strutturale e Stereochimica Inorganica e Centro CNR, Università di Milano,
Via Venezian 21, 20133 Milano, Italy
Fax: (internat.) +39-02/7063-5288,
E-mail: norbert@csmtbo.mi.cnr.it
[b] Dipartimento di Scienze Chimiche, Fisiche e Matematiche, Università dell'Insubria,
via Valleggio 11, 22100 Como, Italy
[c] Dipartimento di Chimica Inorganica, Metallorganica ed Analitica e Centro CNR, Università di Milano,
Via Venezian 21, 20133 Milano, Italy

  1434–1948/00/1212–2507 $ 17.50+.50/0 

**2b**, and $Zn(pymo)_2$, **1c**. The water content in complex **2b** has been verified by TGA analyses, which indicated that all the water molecules are lost in a one-step process at relatively low temperature (200 °C, vide infra) giving rise to the anhydrous species $Ni(pymo)_2$, **1b**.

The synthesis of the hydrazine derivatives $M(pymo)_2(NH_2NH_2)_2$ (M = Ni, Co, Zn) originally derives from the failure in attempting the synthesis of cobalt(I) species by one electron reduction of cobalt(II) in the $Co(pymo)_2$ derivative **1a** with $NH_2NH_2$. The formation of the unexpected $Co(pymo)_2(NH_2NH_2)_2$ species, **3a**, prompted us to thoroughly investigate this complex and to verify if such a reaction could also occur for the nickel and zinc pyrimidin-2-olate derivatives. Consistently, all three species $M(pymo)_2$ easily react with $NH_2NH_2$ in acetonitrile, giving rise to derivatives of general formula $M(pymo)_2(NH_2NH_2)_2$ (M = Co, **3a**; Ni, **3b**; Zn, **3c**).

### Crystal Structures of $Co(pymo)_2$ (1a) and $Zn(pymo)_2$ (1c)

The isomorphous crystals of **1a** and **1c** contain tetrahedrally coordinated metal(II) ions (lying on a −4 symmetry site, *a* in Wyckoff notation), which are linked to four nitrogen atoms of distinct pymo ligands [Co−N = 2.032(4) Å, Zn−N = 2.086(4) Å]. A schematic drawing of the crystal packing, viewed approximately down [001], is shown in Figure 1. As already observed in several group 11 derivatives, pymo ligands coordinate in the common *N,N′*-exobidentate mode ($\mu_2$-$\eta^1$-$\eta^1$ coordination), bridging metal atoms which are 5.65 (Co) or 5.70 Å (Zn) apart.[14] In the crystals, all ligands lie about twofold axes (*d* in Wyckoff notation), passing through the C=O vector and parallel to *a* (and *b*).

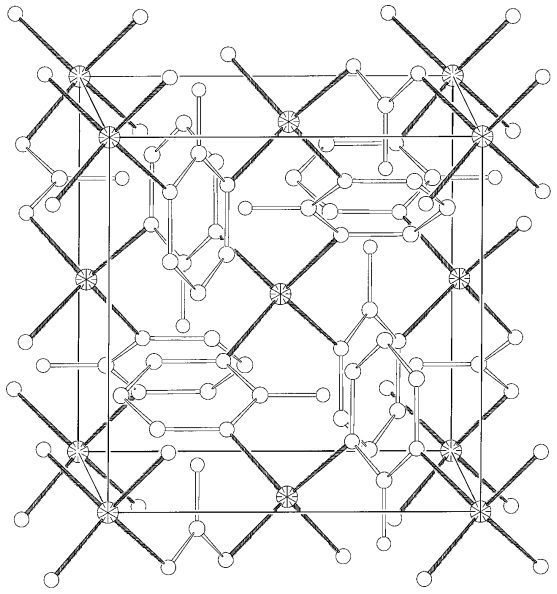

Figure 1. Crystal packing of species **1a**, viewed approximately down [001]; metal atoms are cross-hatched

Disregarding the actual shape of the ligands, the topology of the overall connectivity is far from unusual, since a non-interpenetrated diamond-like framework can be easily recognized. However, it is rather surprising that simple(r) metal diazolates, which contain tetrahedral ions and N,N′ exobidentate $C_{2v}$ anionic heterocycles (i.e. ligands of similar steric, electronic, and symmetry requirements) do not afford the highly symmetric structure found for **1a**; indeed, up to eight crystallographically independent imidazolate (imz) ligands (average Co−N distance: 1.984 Å) are found in $Co(imz)_2$.[15] Similarly, cobalt and zinc pyrazolates (pz), where much shorter M···M contacts are present,[16] do not afford three-dimensional diamondoid structures, but, albeit maintaining tetrahedral coordination, only exist as linear chain (1-D) polymers. However, it must be noted that many of these species are prone to extended polymorphism [see for example Cu(pz),[6] Ag(pz),[6] $Cu(imz)_2$[17] and $Pt(pz)_2$[18]], and that the occurrence of one crystal phase cannot rule out the possibility of a different polymorph.

### Crystal Structure of $Ni(pymo)_2$ (1b)

A schematic drawing of the crystal packing of **1b**, viewed down [001] is shown in Figure 2. Bearing in mind that a body-centered tetragonal cell can be always described by a F-centered tetragonal lattice with twice the volume, one can see that the structure of **1b**, in the observed *Fdd*2 space group (after axis relabelling) bears a proper subgroup relation to that of **1a**, (*I*-42*d*) and, therefore, suggests that **1b** can be obtained by removing a symmetry element (in this case, the −4 improper rotation) from the highly symmetric crystals of **1a**. Indeed, crystals of **1b** contain nickel(II) ions (lying on twofold axes, *a* in Wyckoff notation) connected to four distinct pymo ligands, with Ni−N values of 2.135(4) and 2.172(4) Å. The removal of the −4 symmetry element is here tentatively explained by the higher tendency of nickel(II), vs. cobalt(II), to hexacoordination,[19] which distorts the original tetrahedral geometry found in **1a** to a $NiN_4$ fragment of approximate saw-horse geometry [*trans* N−Ni−N value: 150.3(9)°], leaving two open coordination sites, now occupied by oxygen atoms of two already coordinated pymo ligands [Ni−O 2.288(6)Å]. Thus, while maintaining the overall (diamondoid) three-dimensional topology found in **1a**, pymo ligands are here found in the *new* $\mu_2$-$\eta^1$-$\eta^2$ coordination mode, i.e. N,O chelating on one side, and purely N donor on the other; the Ni···Ni interatomic distance, bridged by such a tridentate pymo ligand, is only 5.46 Å. The overall coordination geometry of each nickel ion is, therefore, best described by *cis*-$NiN_4O_2$ pseudooctahedral fragments, their refined bond lengths and angles being reported in the caption of Figure 2. It is noteworthy that the coexistence of N and $\eta^2$-*N,O* coordination at the same metal has been previously found for the $[Cu(Hpymo)_4]^{2+}$ cation,[20] with the notable difference that, although maintaining crystallographically imposed $C_2$ symmetry, the oxygen atoms in the latter occupy *trans*, rather than *cis*, positions.

### Crystal Structure of $Ni(pymo)_2(H_2O)_{2.5}$ (2b)

Crystals of **2b** contain octahedrally coordinated nickel(II) ions (lying on a crystallographic −1 site symmetry position, *e* in Wyckoff notation), bonded to four nitrogen atoms of four distinct pymo ligands and two mutually *trans* water

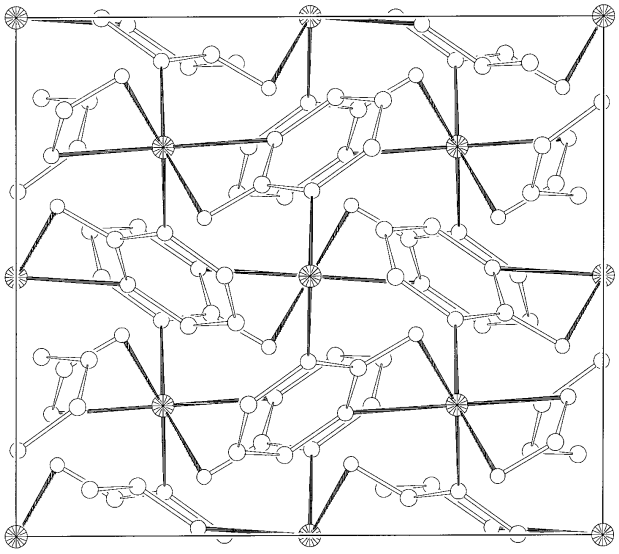

Figure 2. Crystal packing of species **1b**, viewed down [001]; metal atoms are cross-hatched

molecules. Additional water molecules, not involved in metal coordination [lying on *2m m* . (Wyckoff's *c*) positions] fill the cavities of the whole framework. Therefore, species **2b** is best represented by the $Ni(pymo)_2(H_2O)_2 \cdot {}^1/_2H_2O$ formulation. A schematic drawing of the crystal packing, viewed approximately down [1−49] is shown in Figure 3. As depicted therein, the pymo ligands act in the *N*,*N*′-exobidentate mode, connecting Ni ions which are 6.33 Å apart (inter alia, the largest distance ever found within such a class of compounds).

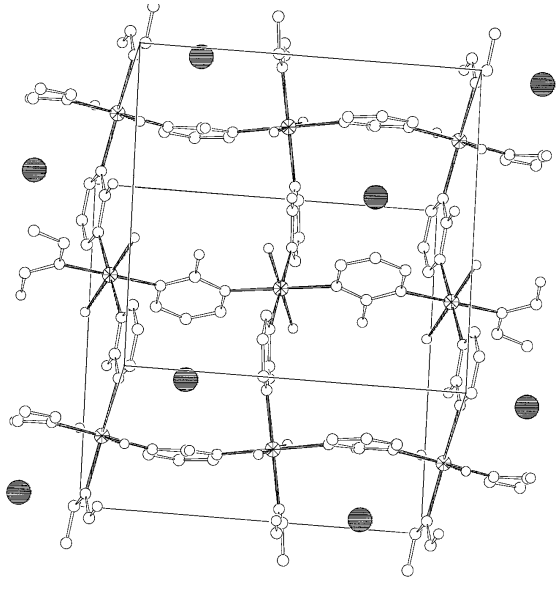

Figure 3. Crystal packing of species **2b**, viewed approximately down [1−49]; metal atoms are cross-hatched, while non-coordinated water molecule are depicted by solid black circles; hydrogen bonds are present, with O···O distances of 2.506(5) and 2.576(3) Å

Neglecting terminally bonded and non-framework water molecules, the overall topology of **2b** can be described by a stack (along *c*) of *two-dimensional* arrays of $Ni(pymo)_2$ squares, thus intrinsically different from the $Co(pymo)_2$ 3-D array described above for **1a**. Interestingly, loosely H-bonded water molecules (O···O >3.0 Å) occupy the cavities of the framework, while much stronger (intralayer, thus "intramolecular") C=O···H−O−H bonds (O···O 2.51−2.58 Å), connecting the pymo oxygens to the coordinated water molecule, are found [and reflected by the significant lowering of the ν(CO) absorption frequency, vide infra].

### Crystal Structures of $Co(pymo)_2(N_2H_4)_2$ (3a), $Ni(pymo)_2(N_2H_4)_2$ (3b), and $Zn(pymo)_2(N_2H_4)_2$ (3c)

Species **3a**, **3b**, and **3c** are strictly isomorphous and contain octahedrally coordinated metal ions. A schematic drawing of the crystal packing, viewed approximately down [108] is shown in Figure 4. Each metal(II) ion lies on a crystallographic *2/m* position (*a* in Wyckoff notation) and is bonded to two (mutually *trans*) oxygen atoms of *mono*dentate ($\mu_1$-$\eta^1$) pymo ligands (slightly off the mirror plane, see Experimental Section) and, equatorially, to four nitrogen atoms of four distinct hydrazine molecules, which bridge metal atoms separated by ca. 4.0 Å (the *b* vector). It is notable that such M···M distances correlate well with the shrinking of the apparent ionic radii on passing from cobalt(II) to zinc(II) ions.

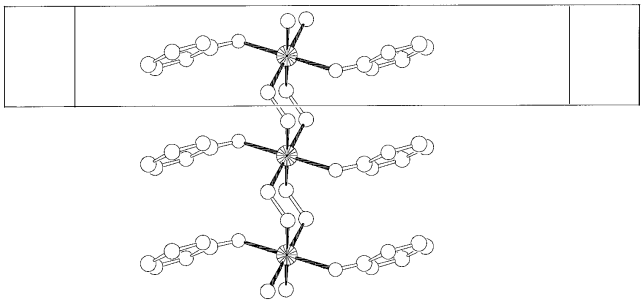

Figure 4. Crystal packing of species **3b**, viewed approximately down [108]; metal atoms are cross-hatched; relevant bond lengths [Å] and angles [°]: Ni−N 2.105(6)−2.111(5), Ni−O 2.208(25); N−Ni−N 89.7(6)−90.3(6), N−Ni−O 89.7(11)−90.3(8)

With reference to Figure 4, one can envisage the existence of linear chains of metal(II) atoms, doubly bridged by $\mu_2$-$N_2H_4$ molecules (in the very same manner as the pyrazolate anion does) and bearing axial monodentate ligands: such a structural pattern is well-known in coordination chemistry, and accounts for a large portion of the known $MX_2L_2$ structures, where M = an octahedrally coordinated dication, X = a bridging anionic ligand (halide, hydroxide, azide) and L = a nitrogen donor neutral ligand.[21]

The most interesting structural features of these species are the monodentate nature of the pymo ligand and the unexpected poly(hydrazine) bridges, which, apparently successfully compete with the propensity of pymo to act as a strong *exo*-bidentate ligand. While the first of these anomalies can be partially understood upon analyzing in detail the environment of the "swinging" end of pymo, for which a number of (weak) N···H−N(hydrazine) bonds is detected (see caption to Figure 4), the formation (and stability) of the $\mu_2$-$N_2H_4$ bridges need more subtle comments.

Hydrazine is known to afford $\mu_2$-bridges, mostly with second and third row transition metals (Ru, Mo, W, Pt), the only structurally characterized species containing a lighter metal being for $Fe^{III}$.[22] Among the known species, a *transoid* form (ideal value of the M−N−N−M torsion angle of 180°) is by far the most commonly observed one. On the other hand, *cis*-M−N−N−M forms are likely to be disfavored by the presence of eclipsed H···H contacts, even if isosteric (and isoelectronic) peroxo fragments bridging octahedrally coordinated metal atoms at distances as low as 4.01 Å are known.[23] These observations, therefore, seem to suggest that there should not be anything special in the formation of a *staggered* M−N−N−M bridge, either *trans* or *gauche* (like in the present case, with a torsion angle near 77°). The peculiar feature in species **3abc** is, however, the presence of an unprecedented[24] bis-dihydrazine link, leading to six-membered M−N−N−M−N−N− *spiro*-rings with chair-like conformation.

### Thermal Stability of Cobalt Derivatives

Powders of **1a** are rather stable and, if heated in a nitrogen atmosphere, only decompose at T > 500 °C, a strongly endothermic peak being observed in the DSC trace near 560 °C. This behaviour is clearly in good agreement with the three-dimensional nature of such coordination polymer, as well as with the negligible tendency of cobalt(II) to display solid-state redox chemistry. In contrast, the much poorer coordination strength of hydrazine speaks for a labile product: indeed, powders of **3a** lose $N_2H_4$ ($t_{1/2}$ a few hours at room temp.), and, surprisingly, quantitatively transform, in the solid, into polycrystalline **1a**. Note that, as discussed below, such transformation requires a dramatic change in the coordination mode of the pymo ligand with heavy shifts (several Å's) of the metal atom locations; nevertheless, it appears to occur without the formation of an (XRPD detectable) intermediate crystalline, or amorphous, material.

### Thermal Stability of Nickel Derivatives

Powders of **2b** lose all water molecules upon heating to almost 200 °C, in a single, nonstructured event, affording a turquoise amorphous powder. Further heating promotes its crystallization (exothermic DSC peak with onset near 315 °C, ca. 26 kJ $mol^{-1}$), forming **1b** in a quantitative manner. Thus the loss of water leaves empty coordination sites and is not immediately accompanied by the 2-D to 3-D structural rearrangement (**2b** => **1b**) which requires extra energy. Interestingly, this transformation leads, from (originally) centrosymmetric crystals, to a conglomerate of enantiomorphic, acentric crystals. Obviously, additional cooling and heating cycles of powders of **1b** (in the 50−400 °C range), did not show any of the aforementioned features. Heating of **1b** at ca. 450 °C in vacuum promotes a *reversible* change of color (green to brown), which may be associated to the formation of tetrahedral nickel(II) ions by labilization of the Ni−O contacts, possibly leading to a tetragonal high-temperature crystal phase isomorphous to **1a** and **1c**, through an easy crystal-to-crystal phase transformation (vide infra).

Species **3b** is rather stable and can be stored under nitrogen indefinitely at room temperature. Contrasting the cobalt analogue, when heated for several hours at 150 °C, **3b** slowly transforms, with hydrazine loss, into a green amorphous material and *does not* form the binary species **1b**, which is, however, restored, as described above for **2b**, upon heating above 320 °C.

### Thermal Stability of Zinc Derivatives

Very similarly to **1a**, and sharing the same crystal structure, species **1c**, upon heating, is rather stable and decomposes near 570 °C, a slightly higher temperature than **1a**. In contrast, species **3c** is rather labile and very rapidly loses $N_2H_4$ ($t_{1/2}$ < 15 min at room temp.) and, as observed for the cobalt analogue, transforms into polycrystalline **1c**. Consistently, this fast loss of hydrazine resulted in an

Table 1. Relevant structural features for compounds **1abc**, **2b**, and **3abc** (e.s.d.'s in parentheses)

| Compound | **1a** | **1b** | **1c** | **2b** | **3a** | **3b** | **3c** |
|---|---|---|---|---|---|---|---|
| Species | $Co(pymo)_2$ | $Ni(pymo)_2$ | $Zn(pymo)_2$ | $Ni(pymo)_2(H_2O)_{2.5}$ | $Co(pymo)_2(N_2H_4)_2$ | $Ni(pymo)_2(N_2H_4)_2$ | $Zn(pymo)_2(N_2H_4)_2$ |
| Site symmetry of M | −4 | 2 | −4 | −1 | −1[a] | −1 | −1 |
| Site symmetry of pymo | 2 | 1 | 2 | *m* | 1[a] | 1 | 1 |
| M···M [Å] | 5.655 | 5.462 | 5.696 | 6.327 | 4.0558(2) | 4.0070(3) | 3.928(2) |
| M−N [Å] | 2.032(4) | 2.172(4)<br>2.135(4) | 2.086(4) | 2.137(6)<br>2.189(1) | n.a.[b] | 2.105(6)[c]<br>2.111(5)[c] | n.a.[b] |
| M−O [Å] | | 2.288(6) | | 2.01(1) | | 2.208(25) | |
| O···O [Å] | | | | 2.506(5)<br>2.576(3) | | | |
| N−M−N [°] | 107.2(1)<br>114.0(3) | 150.3(9), *trans*<br>96.8(5)−109.8(2), *cis* | 108.0(1)<br>112.5(2) | | | 89.5(5)<br>90.5(5) | |
| Coordination mode of pymo | $\mu_2$-$\eta^1$-$\eta^1$(*N*,*N'*) | $\mu_2$-$\eta^2$-$\eta^1$[(*N*,*O*),*N'*)] | $\mu_2$-$\eta^1$-$\eta^1$(*N*,*N'*) | $\mu_2$-$\eta^1$-$\eta^1$(*N*,*N'*) | $\eta^1$(*O*) | $\eta^1$(*O*) | $\eta^1$ (O) |
| ν(CO) [$cm^{-1}$] | 1630 | 1586 | 1633 | 1605 | | 1223 | |
| Color | pink (fuchsia) | green | white | turquoise | pale pink | pale violet | white |

[a] For **3abc**, the site symmetry of an *ideally ordered* crystal phase is quoted (see *Experimental*). − [b] Structures not refined (isomorphous with **3b**). − [c] Subjected to restraints.

XRPD pattern of low(er) quality, for it shows a multiphase system (evolving with time), measured, in order to avoid complete decomposition, over a short time.

### Infrared Spectroscopy

Infrared spectra of complexes **1abc**, **2b**, and **3abc** display the versatility of the coordination features of the pymo ligand. In particular, the position of the ν(CO) band of the lactamic form can be employed as a useful diagnostic tool in order to establish the coordination mode of the ligand (see Table 1).

Derivatives **1a** and **1c** show ν(CO) absorptions at relatively high wavenumbers (1630 and 1633 $cm^{-1}$, respectively), in agreement with the *N*,*N* coordination of the pyrimidin-2-olate ligand and the absence of any interaction between the exocyclic oxygen and the metal centers.[25] Complex **2b** exhibits such a ν(CO) absorption at 1605 $cm^{-1}$. The shift can be justified by the presence of strong hydrogen-bonds between coordinated water and the carbonyl moiety. Moreover, complex **2b** also shows two strong and broad absorptions centered at 2900 and 2250 $cm^{-1}$. These bands are often found in species possessing strong *intra-* or *inter*molecular hydrogen bonds, e.g. in a large series of pyrazole/pyrazolate derivatives.[26] After removal of coordinated and clathrated water from **2b** (obtaining **1b)**, the aforementioned bands disappear and the ν(CO) absorption shifts at 1586 $cm^{-1}$, in agreement with the presence of the M···O=C interaction depicted above.

Given the poor stability at ambient conditions of species **3a** and **3c**, only the hydrazine adduct of the $Ni(pymo)_2$ species can give spectroscopic information about the coordination mode of pymo. Indeed, in **3b**, the aforementioned ν(C=O) bands near 1600 $cm^{-1}$ are absent, while a strong absorption, not present in **1abc** or **2b**, is found at 1223 $cm^{-1}$, which can be attributed to the C−O stretching (of single-bond character) of the pymo ligand coordinating as a phenolate (vide supra).

| METAL (M) | ENVIRONMENT AROUND THE METAL | | |
|---|---|---|---|
| Co, (**1a**) Zn, (**1c**) | $M(N)_4$ | 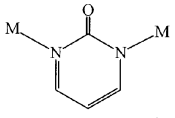 | 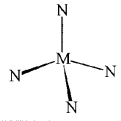 |
| Ni, (**2b**) | $M(N)_4(O_W)_2$ | 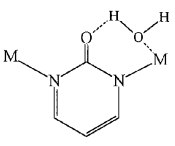 | 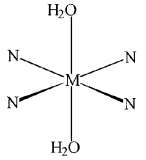 |
| Ni, (**1b**) | $M(N,O)_2(N)_2$ | 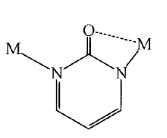 | 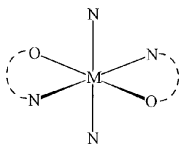 |
| Co, (**3a**) Ni, (**3b**) Zn, (**3c**) | $M(O)_2(N_{idr})_4$ | 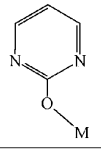 | 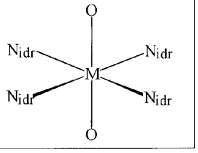 |

Scheme 2

Scheme 2 also summarizes the structural and spectroscopic information discussed above.

## Discussion

All $M(pymo)_2$ phases presented above crystallize in non-centrosymmetric space groups and contain aromatic *dipolar* fragments of idealized $C_{2v}$ symmetry with highly delocalized π electrons. Therefore, in agreement with recent studies on $C_{2v}$ DCM laser dye derivatives[27] and diazaaromatic metal complexes,[28] they are ideal candidates for testing NLO properties, such as second harmonic generation activity.[29] Preliminary measurements ($\lambda_{exc}$ = 1064 nm) by the Kurtz−Perry technique[30] have indeed shown SHG efficiencies of about 5, 8, and 0.2% (urea as standard) for **1a**, **1b**, and **1c**, respectively.

In addition, they all display rather stable three-dimensional frameworks, which do not decompose or melt upon heating at 500 °C; compared to the other known metal(II) diazolates, they show the highest stabilities: indeed, only $Zn(pz)_2$ was found to sustain rather high temperatures (although decomposing near 440 °C to crystalline zinc dicyanide, with selective $CH_3CN$ extrusion), while accessibility to redox reactions [such as cyanogen formation for $Cd(pz)_2$ or ring mercuriation for $Hg(pz)_2$] dramatically lowers the thermal stability of such species,[16b] including $Cu(4X\text{-}pz)_2$. (X = H, Br, Cl, $CH_3$)[31] and $Cu(imz)_2$.[17] That pymo ligands form rather stable metal adducts was already observed for copper(I) and silver(I) ions: indeed, Cu(pymo)[32] decomposes 70 °C higher than α-Cu(pz)[33] (dec. 270 °C) and *hexameric* Ag(pymo) is stable up to 300 °C,[34] about 40 °C higher than the Ag(pz)[33] and Ag(imz)[35] *polymers.*

Interestingly, while in the previously known silver and copper pyrimidinolates, the pymo ligand was exclusively found to coordinate in the $\mu_2$-$\eta^1$-$\eta^1$ (*N*,*N*′) mode, the structures reported in this paper demonstrate its coordination versatility. Indeed, within a homogeneous class of compounds, pymo acts either as a ($\mu_1$-$\eta^1$-*O*) monodentate or as a (*N*,*N*′) polydentate ligand, with ($\mu_2$-$\eta^2$-$\eta^1$) or without ($\mu_2$-$\eta^1$-$\eta^1$) ancillary oxygen coordination.[36] In contrast, the isostructural pyrimidin-2-thiolato ligand, which, owing to the biological importance of its derivatives,[37] has been extensively characterized in a large number of metal complexes, has never been found in the pure $\mu_2$-$\eta^1$-$\eta^1$ (*N*,*N*′) mode, but, in the rare cases where both N atoms were involved in metal coordination,[38] the (larger and softer) sulfur atom was invariably found in the coordination sphere of one metal.

The different bridging modes of the pymo ligand also influence the distances at which nearest M···M contacts are found: they surprisingly range from 5.46 to 5.70 Å for the binary species up to ca. 6.33 Å for the octahedrally coordinated nickel(II) ions in the hydrated species **2b**. Consistently, the flexibility of such links affects not only the different

connectivity patterns described above, but also the actual values of the M−N and M−N−C bond lengths and angles (see Table 1).

## Conclusions

In this paper we have demonstrated that reaction of metal ions with deprotonated diazaaromatic ligands can afford rather stable coordination polymers, which can be heated without decomposition up to ca. 550 °C. When pymo and Co, Ni, and Zn ions are employed, three-dimensional diamondoid networks are formed, in contrast with the 1-D nature of all known $M(pz)_2$ polymers (M = Cu, Zn, Cd, Hg). Such stereochemical features, together with the low(er) propensity of Co, Ni and, particularly, Zn toward redox reactions, are thought to heavily influence the stability of such crystal phases. In the process of developing suitable syntheses for such species, a number of water and hydrazine adducts have been prepared, the structural characterization of which showed the extreme versatility of the pymo ligands, as well as the formation of 2-D (for **2b**) and 1-D (**3abc**) polymers.

Since all these species could only be obtained as microcrystalline samples, their full structural analyses was performed through the ab initio XRPD technique (see Appendix); as recently shown by us in the field of coordination chemistry for metal pyrazolates and metal diazaaromatic halides, this method has become a powerful laboratory tool for the complete characterization of *entire* classes of compounds and not only, as often appeared in the recent literature, for fortunate, isolated or benchmark cases bearing methodologically important aspects.

## Experimental Section

**General:** 2-Hydroxypyrimidine hydrochloride and metal salts were used as supplied (Aldrich Chemical Co.). − Infrared spectra were recorded on a BIO RAD FTIR 7 instrument. − Thermogravimetric analyses were performed on a Perkin−Elmer TGA-7 system. DSC traces were obtained with the aid of a Perkin−Elmer DSC 7 calorimeter. − X-ray powder diffraction was used to characterize the phases formed upon heating the powders in the DSC furnace. − Elemental analyses (C, H, N) were carried out at Microanalytical Laboratory of the University of Milan.

**Synthesis of Cobalt(II), Nickel(II), and Zinc(II) Derivatives:** Complexes **1a**, **2b**, and **1c** have been prepared following the same synthetic route: ten mmol of the appropriate metal chloride ($CoCl_2{\cdot}6H_2O$, 2.38 g, $NiCl_2{\cdot}6H_2O$, 2.38 g and $ZnCl_2$, 1.36 g) were dissolved in distilled water (30 mL) and 2-hydroxypyrimidine hydrochloride (3.31 g, M/Hpymo ratio = 1:2.5) was added under stirring. The clear solutions were kept at room temperature for about 20 min., then the temperature was raised to 90 °C and aqueous ammonia (25% w/w) was added dropwise, adjusting the pH of the solution to a value near 10. The pink $Co(pymo)_2$, **1a**, and the white $Zn(pymo)_2$ species, **1c**, suddenly precipitate, whereas turquoise $Ni(pymo)_2(H_2O)_{2.5}$, **2b**, separates from a deep blue solution in about 10 minutes. The suspensions were stirred at 90 °C for an additional half hour, the solids were then filtered, washed with hot water and dried under vacuum.

**Anhydrous $Ni(pymo)_2$, 1b**, (amorphous phase) was obtained upon heating the hydrated $Ni(pymo)_2(H_2O)_{2.5}$ species **2b** at 200 °C for 10 min under vacuum. A microcrystalline powder of **1b**, suitable for the XRPD study (vide infra), was obtained after over-heating the solid at ca. 550 °C under vacuum. All preparations gave quantitative (>95%) yields. Analyses: **1a**: $C_8H_6CoN_4O_2$: calcd. C 38.57, H 2.41, N 22.49; found C 38.51, H 2.47, N 22.41; **1b**: $C_8H_6N_4NiO_2$: calcd. C 38.60, H 2.41, N 22.52; found C 38.53, H 2.45, N 22.45; **1c**: $C_8H_6N_4O_2Zn$: calcd. C 37.59, H 2.35, N 21.93; found C 37.47, H 2.43, N 21.86; **2b**: $C_8H_{11}N_4NiO_{4.5}$: calcd. C 32.69, H 3.75, N 19.07; found C 31.91, H 3.85, N 18.85.

**Synthesis of the Hydrazine Adducts:** Complexes **1a** (or **1b/1c**) (500 mg, about 2 mmol) were suspended in acetonitrile (7 mL) and hydrazine (160 μL, 80% water solution) was added with stirring. A rapid change in color was observed when cobalt or nickel pyrimidin-2-olate derivatives were employed (from pink to white and from turquoise to very light violet, respectively). The suspensions were stirred for 4 h, the solids were then filtered under nitrogen (to avoid atmospheric moisture) and dried under a flow of dry nitrogen. The nickel derivative $Ni(pymo)_2(N_2H_4)_2$, can also be obtained employing $Ni(pymo)_2(H_2O)_{2.5}$ in place of $Ni(pymo)_2$. A longer reaction time is in this case required (about 12 h). Analysis for **3b**: $C_8H_{14}N_8NiO_2$: calcd. C 30.70, H 4.48, N 35.82; found C 30.77, H 4.41, N 35.73; due to thermal instability, the chemical analyses for **3a** and **3c** are erratic (see text).

**X-ray Powder Diffraction Analysis of 1abc, 2b, and 3abc:** The powders were gently ground in an agate mortar, than cautiously deposited in the hollow of an aluminium holder equipped with a zero background plate (supplied by The Gem Dugout, State College, PA) with the aid of glass slide. Diffraction data (Cu-$K_\alpha$, $\lambda$ = 1.5418 Å) were collected on a vertical scan Philips PW1820 diffractometer, equipped with parallel (Soller) slits, a secondary beam curved graphite monochromator, a Na(Tl)I scintillation detector and pulse height amplifier discrimination. The generator was operated at 40 KV and 40 mA. Slits used: divergence 1.0°, antiscatter 1.0° and receiving 0.2 mm. Nominal resolution for the present setup is 0.12° 2θ (FWHM) for the Si(111) peak at 28.44° (2θ). Long overnight scans were performed for **1abc**, **2b**, and **2c** with $5<2\theta<95°$, with $t$ = 10 s and $\Delta 2\theta$ = 0.02°, while the low stability of the zinc hydrazine adduct required a much faster scan ($5<2\theta<35°$, $t$ = 1s, approximately 30 min long).

Indexing, using TREOR,[39] of the low angle peaks suggested, for **1a** and **2b**, tetragonal unit cells of approximate dimensions $a$ = 7.39, $c$ = 17.03 Å for **1a** [M(20)[40] = 19; F(20)[41] = 25 (0.016, 51), I-centered] and $a$ = 12.62, $c$ = 14.54 Å for **2b** [M(10) = 32; F(10) = 38 (0.012, 22), primitive]; in contrast, the unit cell determination of **3a** lead to a triclinic cell [$a$ = 4.04, $b$ = 6.04, $c$ = 15.42 Å, α = 64.3, β = 113.3 and γ = 90.4°; M(13) = 24; F(13) = 35 (0.015, 24)], which could be successfully transformed into a C-centered monoclinic lattice with $a$ = 25.04, $b$ = 4.04, $c$ = 6.04 Å, β = 92.8°; indexing of **1b** suggested, as probable unit cell, an orthorhombic lattice with $a$ = 11.02, $b$ = 9.60 Å, $c$ = 16.21, [M(11) = 23; F(11) = 29 (0.006, 67); F-centered]. Systematic absences indicated (among others) *I−42d*, *C2/m*, *$P4_2$/nmc*, and *Fdd2* as the probable space group, for **1a**, **3a**, **2b**, and **1b**, respectively, later confirmed by successful solution and refinement; **3b** and **3c** were found to be strictly isomorphous with **3a** (and **1c** to **1a**), and, therefore, not solved ab initio.

Structure solutions of **1a**, **1b**, and **2b** were initiated by EXPO[42] [108 ($2\theta<85°$), 147 and 84 ($2\theta < 65°$) independent $F_o$'s, respectively]

which afforded all metal and N atom locations, as well as the positions of a few other light atoms. With the help of difference Fourier syntheses and geometrical modeling, approximate coordinates for the remaining non-hydrogen atoms were easily obtained. Approximate lattice constants and atomic coordinates for **1c** were taken from those of the isomorphous species **1a**.

In contrast, the structure of **3abc** could not solved by this method; therefore, we resorted to the ′brutal force′ program ESPOIR,[43] which combines direct space search and a reverse Monte Carlo algorithm; rather efficiently, using 134 $F_o$'s extracted by EXPO, this program succeeded in finding the Ni atom in **3b** and approximate location and orientation of the (crystallographically unique) pymo ligand. Difference Fourier and geometric modeling later afforded the location of $\mu_2$-bridging hydrazine. However, the original location of the pymo and hydrazine ligands, bisected by crystallographic mirror planes, afforded reasonable profile agreement factors ($wR_p$ and $R_p$: 0.175 and 0.132, respectively), but a poor $R_F$ value (0.184) and a rather strained hydrazine molecule, possessing an implausible *eclipsed* conformation and N−N−Co angles near 135°. Therefore, we suspected the presence of local disorder of the hydrazine bridges and simulated the diffraction pattern for ordered and disordered C-1 and C2 models. Comparison of the Rietveld refinements, of the resulting stereochemistries and evaluation of the overall (intramolecular + packing) steric energy by a locally developed molecular mechanics programs (based on the MM3 force field and capable of dealing with crystal lattices and polymeric systems[44]), revealed that *disordered* bis-hydrazine bridges, with M−N−N−M−N−N rings in chair conformation, and pymo ligands slightly off the mirror plane, are present, with the strict stereochemical condition that, within each polymeric chain, a rather perfect order is maintained, and that the average *C2/m* space group symmetry stems from the order loss in the lateral packing of chains. Therefore, the final model described in the following, as well in Table 1 and Table 2, Figure 5 and in the Supporting Information, show split ligands with atomic fractional occupancy of 0.5.

The final refinements were performed with the aid of the GSAS suite of programs,[45] by imposing steric restraints to chemically stiff and known fragments: pymo rings were idealized with average literature values (C−C and C−N: 1.38 Å; C=O: 1.25 Å; all angles set at 120°). A soft restraint was also applied to hydrazine N−N distance [1.44(1) Å in **3b**]. The peak shapes were best described by the Thompson/Cox/Hastings formulation[46] of the pseudo Voigt function, with GV and LY set to zero. The experimental background was modeled by a cosine Fourier series, while systematic errors were corrected with the aid of a sample-displacement angular shift. Metal atoms were given a refinable isotropic displacement parameter [$U_{iso}$(M)], while lighter atoms *U*'s were arbitrarily given [$U_{iso}$(M) + 0.02] Å$^2$ values. The contribution of the hydrogen atoms to the scattered intensity was neglected. Scattering factors, corrected for real and imaginary anomalous dispersion terms, were taken from the internal library of GSAS. Final $R_p$, $R_{wp}$, and $R_F$ agreement factors, together with details of the data collections and analyses for the seven crystal phases can be found in Table 2. Figure 5 shows the final Rietveld refinement plots. The multiphase nature *and* the variable composition of the XRPD data for species **3a** and **3c** prevented a full structural refinement; therefore, the data reported in Table 2 refer to a LeBail (**3a**) and multiple peak positions (**3c**), rather than Rietveld, fit. Final fractional coordinates and full lists of bond lengths and angles are supplied as Supporting Information. Crystallographic data (excluding structure factors) for the structures reported in this paper have been deposited with the Cambridge Crystallographic Data Centre as supplementary publication no. CCDC-141485−141489. Copies of the data can be obtained free of charge on application to CCDC, 12 Union Road, Cambridge CB2 1EZ, UK [fax: (+44)1223 336−033; E-mail: deposit@ccdc.cam.ac.uk].

## Appendix

X-ray powder diffraction is known to afford very good estimates of the lattice parameters, but only approximate values for atomic position and thermal displacement parameters. Also, in the formulation of the ′correct′ structural model for complex structures, *external* knowledge, such as chemical composition and stereochemical rules, must be introduced by the sagacious use of restraints. We

Table 2. Crystal data and refinement parameters for compounds **1abc**, **2b**, and **3abc** (e.s.d.'s in parentheses)

| Compound | **1a** | **1b** | **1c** | **2b** | **3a** | **3b** | **3c** |
|---|---|---|---|---|---|---|---|
| Species | $Co(pymo)_2$ | $Ni(pymo)_2$ | $Zn(pymo)_2$ | $Ni(pymo)_2(H_2O)_{2.5}$ | $Co(pymo)_2(N_2H_4)_2$ | $Ni(pymo)_2(N_2H_4)_2$ | $Zn(pymo)_2(N_2H_4)_2$ |
| Formula | $C_8H_6CoN_4O_2$ | $C_8H_6N_4NiO_2$ | $C_8H_6N_4O_2Zn$ | $C_8H_{11}N_4NiO_{4.5}$ | $C_8H_{14}CoN_8O_2$ | $C_8H_{14}N_8NiO_2$ | $C_8H_{14}N_8O_2Zn$ |
| *Fw* [g mol$^{-1}$] | 249.09 | 248.87 | 255.33 | 293.91 | 313.18 | 312.97 | 319.62 |
| Crystal system | Tetragonal | Orthorhombic | Tetragonal | Tetragonal | Monoclinic | Monoclinic | Monoclinic |
| Space Group | *I*-42*d* | *Fdd*2 | *I*-42*d* | $P4_2/nmc$ | *C*2/*m* | *C*2/*m* | *C*2/*m* |
| *a* [Å] | 7.4114(3) | 11.0361(6) | 7.3919(2) | 12.6531(4) | 25.139(2) | 25.237(5) | 25.40(1)[b] |
| *b* [Å] | 7.4114(3) | 9.6611(8) | 7.3919(2) | 12.6531(4) | 4.0558(2) | 4.0070(4) | 3.928(2) |
| *c* [Å] | 17.0879(7) | 16.1935(8) | 17.3389(6) | 14.5844(9) | 6.0752(4) | 6.0580(7) | 6.163(3) |
| α [°] | 90 | 90 | 90 | 90 | 90 | 90 | 90 |
| β [°] | 90 | 90 | 90 | 90 | 92.813(4) | 93.156(9) | 93.06(4) |
| γ [°] | 90 | 90 | 90 | 90 | 90 | 90 | 90 |
| *V* [Å$^3$] | 938.63(6) | 1726.6(2) | 947.39(5) | 2335.0(2) | 618.66(8) | 611.7(2) | 614.2(6) |
| *Z* | 4 | 8 | 4 | 8 | 2 | 2 | 2 |
| $\rho_{calc}$ [g cm$^{-3}$] | 1.763 | 1.915 | 1.791 | 1.669 | 1.681 | 1.704 | 1.729 |
| μ(Cu-$K_\alpha$) [cm$^{-1}$] | 149.4 | 31.0 | 35.4 | 25.4 | 115.5 | 24.1 | 29.5 |
| Diffractometer | Philips PW 1820 | Philips PW 1820 | Philips PW 1820 | Philips PW 1820 | Philips PW 1820 | Philips PW 1820 | Philips PW 1820 |
| *T* [K] | 298 | 298 | 298 | 298 | 298 | 298 | 298 |
| 2θ range ° | 12−90 | 10−95 | 10−95 | 5−95 | 5−65 | 5−65 | 5−35 |
| $N_{obs}$ | 3900 | 4250 | 4250 | 4500 | 3000 | 3000 | 1500 |
| $N_{refl}$ | 120 | 204 | 135 | 600 | 131 | 142 | n.a. |
| $R_p$, $R_p$ | 0.103, 0.078 | 0.090. 0.066 | 0.121, 0.088 | 0.199, 0.142 | 0.100, 0.072[a] | 0.125, 0.089 | n.a. |
| $R_F$, χ | 0.076, 2.92 | 0.051, 1.55 | 0.096, 2.54 | 0.129, 3.67 | n.a. | 0.069, 2.86 | n.a. |

[a] From a model-independent LeBail fit. − [b] From 14 single-peak locations, using UNITCELL (Toraya, H.; Kitamura, M.; *J. Appl. Crystallogr.*, **1990**, *23*, 282.)

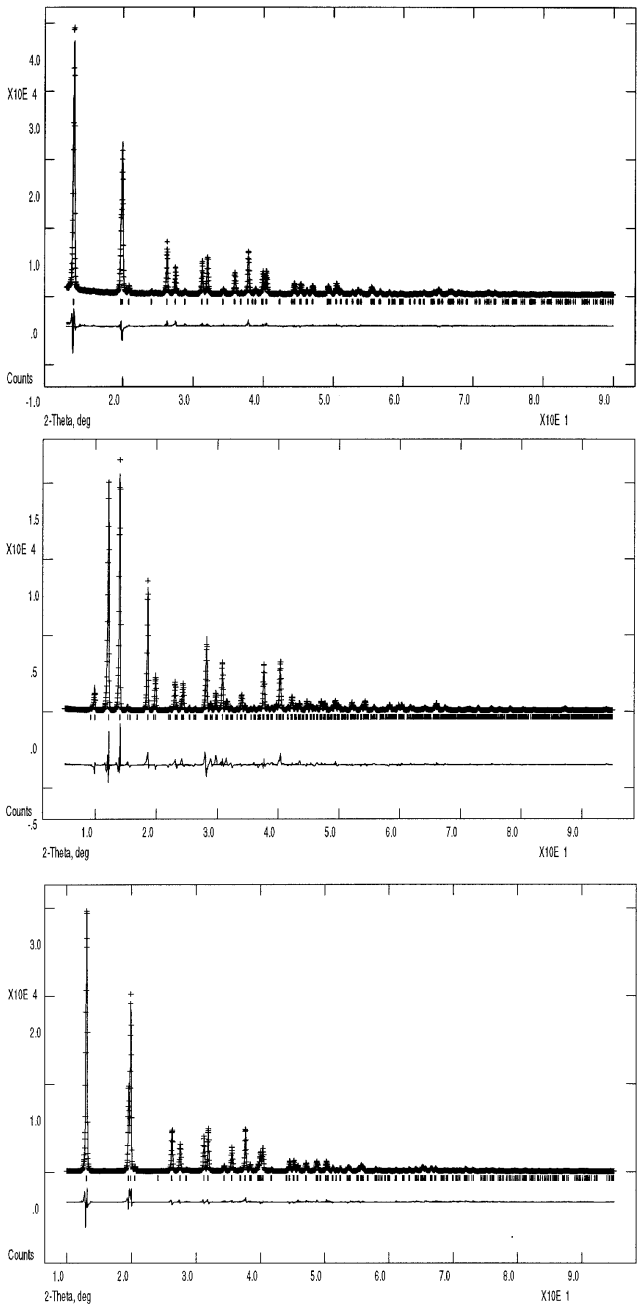


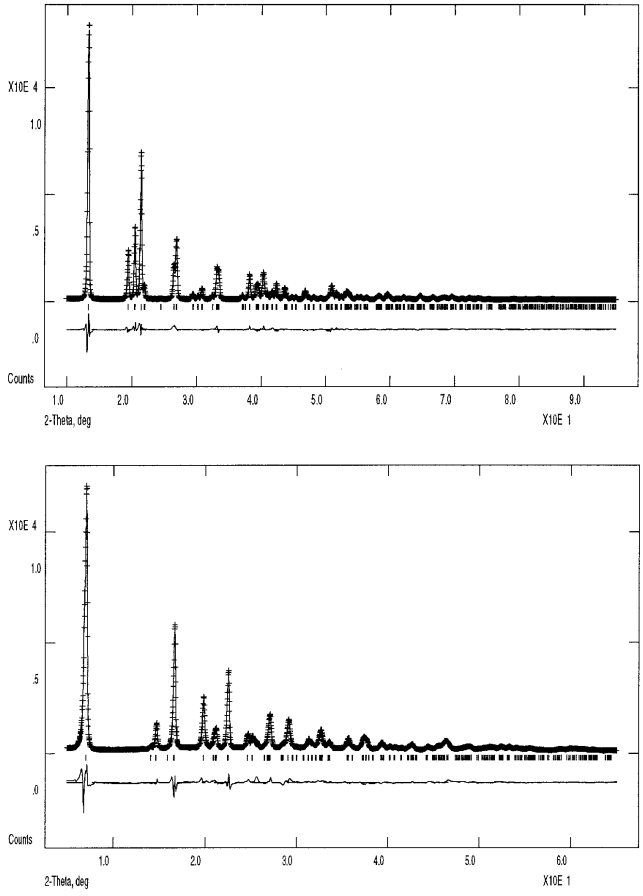


Figure 5. Rietveld Refinement plots for species **1a**, **1b**, **1c**, **2b**, and **3b** (top to bottom, left to right), respectively; peak markers and difference plot at the bottom

have recently demonstrated that packing energy evaluation within the crystal lattice may discriminate among similar models, thus acting as a lens for rescuing subtle details at spatial resolution higher that that affordable by XRPD data alone.[47] Accordingly, the final structural model for species **3b** has been derived after *overall* steric energy minimization, stereochemical considerations and a number of parallel refinements had been performed, with the aim of identifying the most likely (i.e. correct?) structural model. While the figures reported hereafter in Table 3 cannot be straightforwardly used as in standard single-crystal diffractometry (apart from the "unobservable" $R_F$ value), it is only their internal comparison and the stereochemical features associated to the different cases that guarantee successful results even from XRPD data.

## Acknowledgments

We thank the Italian Consiglio Nazionale delle Ricerche and MURST for funding. We also acknowledge financial support from

Table 3. Comparison of Rietveld refinements for **3b**, in the 5−65° (2θ) range (fixed cell)

| | Model | S.G. | $N_{parameters}$ | $N_{restraints}$ | $wR_p$ | $R_p$ | $R_F$ | $N_{ref}$ |
|---|---|---|---|---|---|---|---|---|
| 1 | ordered | *C*−1 | 40 | 19 | 0.139 | 0.105 | 0.108 | 222 |
| 2 | ordered | *C*2 | 40 | 19 | 0.141 | 0.104 | 0.092 | 141 |
| 3 | ordered (N−N free) | *C*2/*m* | 30 | 16 | 0.146 | 0.108 | 0.162 | 141 |
| 4 | as 3 (N−N 1.44 Å) | *C*2/*m* | 30 | 17 | 0.175 | 0.132 | 0.184 | 141 |
| 5 | disordered | *C*2/*m* | 40 | 19 | 0.126 | 0.093 | 0.082 | 141 |

ICDD − International Centre for Diffraction Data. The help of E. Cariati for the SHG measurements is also acknowledged.


[1] J. E. Mark, H. R. Allcock, R. West, *Inorganic Polymers*, Prentice-Hall Inc., Englewood Cliffs, NJ, **1992**; *Inorganic and Organometallic Polymers II* (Eds. P. Wisian-Neilson, H. R. Allcock, K. J. Wynne), ACS Symposium Series 572, American Chemical Society, Washington, DC, **1994**.

[2] O. Kahn, C. Jay Martinez, *Science* **1998**, *279*, 44−48 and references therein.

[3] I. V. Tsarenko, A. V. Makarevich, T. P. Kofman, *Russian J. Electrochem.* **1997**, *33*, 1092−1097; W. N. Richmond, P. W. Faguy, S. C. Weibel, *J. Electroan. Chem.* **1998**, *448*, 237−244; I. V. Tsarenko, S. A. Chizhik, A. V. Makarevich, *Protect. Met.* **1999**, *35*, 81−84.

[4] K. Nomiya, K. Tsuda, T. Sudoj, M. Oda, *J. Inorg. Biochem.* **1997**, *68*, 39−44; K. Nomiya, K. Tsuda, N. C. Kasuga, *J. Chem. Soc., Dalton Trans.* **1998**, 1653−1659.

[5] A. J. Blake, N. R. Champness, P. Hubberstey, W. S. Li, M. A. Withersby, M. Schröder, *Coord. Chem. Rev.* **1999**, *183*, 117−138.

[6] N. Masciocchi, M. Moret, P. Cairati, A. Sironi, G. A. Ardizzoia, G. LaMonica, S. Cenini, *J. Am. Chem. Soc.* **1994**, *116*, 7668−7676.

[7] [7a]N. Masciocchi, G. A. Ardizzoia, G. LaMonica, M. Moret, A. Sironi, *Inorg. Chem.* **1997**, *36*, 449−454. − [7b] N. Masciocchi, P. Cairati, A. Sironi, *Powder Diffr.* **1998**, *13*, 35−40. − [7c] G. A. Ardizzoia, S. Cenini, G. LaMonica, N. Masciocchi, A. Maspero, M. Moret, *Inorg. Chem.* **1998**, *37*, 4284−4292.

[8] N. Masciocchi, M. Moret, P. Cairati, A. Sironi, G. A. Ardizzoia, G. La Monica, *J. Chem. Soc., Dalton Trans.* **1995**, 1671−1675.

[9] M. Quiros, *Acta Crystallogr.* **1994**, *C50*, 1236−1238.

[10] N. Masciocchi, E. Corradi, M. Moret, G. A. Ardizzoia, A. Maspero, G. LaMonica, A. Sironi, *Inorg. Chem.* **1997**, *36*, 5648−5650.

[11] N. Masciocchi, G. A. Ardizzoia, G. LaMonica, A. Maspero, A. Sironi, *Angew. Chem. Int. Ed.* **1998**, *37*, 3366−3369.

[12] K.D.M. Harris, M. Tremayne, *Chem. Mater.* **1996**, *8*, 2554−2570; J. I. Langford, D. Louër, *Rep. Prog. Phys.* **1996**, *59*, 131−234; D. M. Poojary, A. Clearfield, *Acc. Chem. Res.* **1997**, *30*, 414−422.

[13] N. Masciocchi, A. Sironi, *J. Chem. Soc., Dalton Trans.* **1997**, 4643−4650.

[14] In contrast to that observed in previous XRPD studies, all M···M separations reported in this paper are rather accurately estimated, since, owing to the special location of the metal atoms, they only depend on the lattice metrics which, from PD experiments, typically possess e.s.d.'s lower than in conventional single-crystal diffractometry.

[15] M. Sturm, F. Brandl, D. Engel, W. Hoppe, *Acta Crystallogr.* **1975**, *B31*, 2369−2378.

[16] [16a]M. Ehlert, A. Storr, R. C. Thompson, *Can. J. Chem.* **1989**, *67*, 1412−1424. − [16b] N. Masciocchi, G. A. Ardizzoia, A. Maspero, G. LaMonica, A. Sironi, *Inorg. Chem.* **1999**, *38*, 3657−3664.

[17] M. Inoue, M. Kishita, M. Kubo, *Inorg. Chem.* **1965**, *4*, 626−628.

[18] W. Bürger, J. Strähle, *Z. Allg. Anor. Chem.* **1985**, *529*, 111−117.

[19] F. A. Cotton, G. Wilkinson, C. A. Murillo, M. Bochmann, *Advanced Inorganic Chemistry*, 6th Edition, Wiley, New York, **1999**, p. 817.

[20] B. A. Cartwright, C. D. Reynolds, A. J. Skapski, *Acta Crystallogr.,* **1977**, *B33*, 1883−1887.

[21] See for example: B. J. Hathaway, *Comprehensive Coordination Chemistry* (Ed.: G. Wikinson), Pergamon, **1987**, vol. 5, p. 599.

[22] D. Sellmann, P. Kreutzer, G. Huttner, A. Frank, *Z. Naturforsch. B* **1978**, *33*, 1341−1346.

[23] K. Kim, S. J. Lippard, *J. Am. Chem. Soc.* **1996**, *118*, 4914−4915.

[24] A very brief report of a ruthenium complex bridged by one disulfide and two hydrazine links has however recently appeared (K. Matsumoto, H. Uemura, M. Kawano, *Chem. Lett.* **1994**, 1215−1218).

[25] For comparison, the ν(CO) of the free Hpymo (lactamic form) is found at 1647 $cm^{-1}$ in the solid state and 1644 $cm^{-1}$ in water solution (A. Albert, E. Spinner, *J. Chem. Soc. A* **1960**, 1221−1226).

[26] G. A. Ardizzoia, G. LaMonica, A. Maspero, M. Moret, N. Masciocchi, *Eur. J. Inorg. Chem.* **1998**, 1503−1512 and references therein.

[27] C. R. Moylan, S. Ermer, S. M. Lovejoy, I.-H. McComb, D. S. Leung, R. Wortmann, P. Krdmer, R. J. Twieg, *J. Am. Chem. Soc.* **1996**, *118*, 12950−12955.

[28] H. Le Bozec, T. Renouard, *Eur. J. Org. Chem.* **2000**, 229−239.

[29] Indeed, a closely related species, 5-nitrouracil (a substituted 2-hydroxypyrimidine), was among the most thoroughly studied crystal phases, with NLO properties similar, or higher in magnitude, than KDP or $LiNbO_3$ [J. F. Nicoud, R. J. Twieg, in *Nonlinear Optical Properties of Organic Molecules and Liquid Crystals* (Eds.: D. S. Chemla, F. Zyss), Academic Press, **1987**, p. 268].

[30] S. K. Kurtz, T. T. Perry, *J. Appl. Phys.* **1968**, *39*, 3798−3813.

[31] M. K. Ehlert, S. J. Rettig, A. Storr, R. C. Thompson, J. Trotter, *Can. J. Chem.* **1989**, *67*, 1970−1974; M. K. Ehlert, A. Storr, R. C. Thompson, F. W. B. Einstein, R. J. Batchelor, *Can. J. Chem.* **1993**, *71*, 331−334; M. K. Ehlert, S. J. Rettig, A. Storr, R. C. Thompson, J. Trotter, *Can. J. Chem.* **1991**, *69*, 432−439.

[32] N. Masciocchi, G. A. Ardizzoia, G. La Monica, A. Maspero, A. Sironi, *Angew. Chem. Int. Ed. Engl.* **1998**, *37*, 3366−3369.

[33] N. Masciocchi, M. Moret, P. Cairati, A. Sironi, G. A. Ardizzoia, G. La Monica, *J. Am. Chem. Soc.* **1994**, *116*, 7668−7676.

[34] N. Masciocchi, E. Corradi, M. Moret, G. A. Ardizzoia, A. Maspero, G. La Monica, A. Sironi, *Inorg. Chem.* **1997**, *36*, 5648−5650.

[35] N. Masciocchi, M. Moret, P. Cairati, A. Sironi, G. A. Ardizzoia, G. La Monica, *J. Chem. Soc., Dalton Trans.* **1995**, 1671−1675.

[36] That pymo ligands could bind also via the oxygen atom was also proposed, from UV/Vis spectroscopic measurements, in: D. M. L. Goodgame, I. Jeeves, *Inorg. Chim. Acta* **1979**, *32*, 157−162.

[37] See for example: J. A. Carbon, L. Hung, D. S. Jones, *Proc. Nat. Acad. Sci.* **1965**, *53*, 979−986; J. A. Carbon, H. David, M. H. Studier, *Science* **1968**, *161*, 1146−1147.

[38] D. R. Corbin, L. C. Francesconi, D. N. Hendrickson, G. D. Stucky, *Inorg. Chem.* **1979**, *18*, 3069−3074; M. L. Godino-Salido, M. D. Gutierrez-Valero, R. Lopez-Garzon, J. M. Moreno-Sanchez, *Inorg. Chim. Acta* **1994**, *221*, 177−181.

[39] P. E. Werner, L. Eriksson, M. Westdahl, *J. Appl. Crystallogr.* **1985**, *18*, 367−370.

[40] P. M. De Wolff, *J. Appl. Crystallogr.* **1968**, *1*, 108−113.

[41] G. S. Smith, R. L. Snyder, *J. Appl. Crystallogr.* **1979**, *12*, 60−65.

[42] A. Altomare, M. C. Burla, G. Cascarano, G. Giacovazzo, A. Guagliardi, A. G. G. Moliterni, G. Polidori, *J. Appl. Crystallogr.* **1995**, *28*, 842−846; A. Altomare, M. C. Burla, M. Camalli, B. Carrozzini, G. L. Cascarano, C. Giacovazzo, A. Guagliardi, A. G. G. Moliterni, G. Polidori, R. Rizzi, *J. Appl. Crystallogr.* **1999**, *32*, 339−340.

[43] A. Le Bail, "http://fluo.univ-lemans.fr:8001/sdpd/espoir/index.html".

[44] P. L. Mercandelli, M. Moret, A. Sironi, *Inorg. Chem.* **1998**, *37*, 2563−2569.

[45] A. C. Larson, R. B. Von Dreele, LANSCE, MS-H805, Los Alamos National Laboratory, New Mexico, **1990**.

[46] P. Thompson, D. E. Cox, J. B. Hastings, *J. Appl. Crystallogr.* **1987**, *20*, 79−83.

[47] N. Masciocchi, F. Ragaini, S. Cenini, A. Sironi, *Organometallics* **1998**, *17*, 1052−1057; N. Masciocchi, A. Sironi, *Adv. X-ray Anal.* **1999**, *42*, 366−372.


Received May 24, 2000
[I00214]